

Toward the Mitigation of Spurious Cloud-Edge Supersaturation in Cloud Models

WOJCIECH W. GRABOWSKI AND HUGH MORRISON

National Center for Atmospheric Research, Boulder, Colorado*

(Manuscript received 14 June 2007, in final form 19 July 2007)

ABSTRACT

This paper presents a straightforward approach to mitigate the problem of spurious cloud-edge supersaturation in high-spatial-resolution cloud models (e.g., moist large-eddy simulation models). The central idea, following a 1989 *J. Atmos. Sci.* paper by Grabowski, is that supersaturation predicted by the supersaturation equation should be used to adjust the temperature and moisture solutions, rather than the other way around as in the standard approach in cloud modeling, where the temperature and moisture solutions are used to diagnose the supersaturation. Details of the adjustment scheme are discussed and illustrated through simple one-dimensional tests applying a two-moment warm-rain microphysics scheme that predicts the in-cloud supersaturation. Extension of this approach to bin microphysics models is also outlined.

1. Introduction

Problems with numerical modeling of cloud processes near sharp cloud–environment interfaces have been long recognized. Klaassen and Clark (1985) were the first to discuss this issue in the context of high-resolution (grid length of a few to a few tens of meters) bulk-model simulations of interfacial instabilities in a small cumulus (see their section 7). The key observation was that deformational flow near the cloud top leads to sharp gradients across the interface and oscillations of the condensation rate. Since the advection scheme applied in their model was not monotone (i.e., advected temperature and moisture variables suffered from dispersive ripples near the interface; see discussion in Smolarkiewicz and Grabowski 1990), the presence of these oscillations was not surprising. Grabowski (1989) extended Klaassen and Clark’s simulations into the case of bin microphysics (condensation–evaporation only) and showed that such problems persist even if a monotone advection scheme is used. In the bin microphysics framework, these problems manifest

themselves in small-scale overshoots of the supersaturation field near cloud edges (see Fig. 7 in Grabowski 1989). To cope with this problem, Grabowski applied a diagnostic approach in which the supersaturation equation was solved by applying a monotone advection scheme, and water vapor was subsequently diagnosed from the predicted supersaturation and temperature fields. Although such an approach produced physically consistent results, a lack of conservation of the total water was a major drawback. The above studies prompted an investigation reported in Grabowski and Smolarkiewicz (1990), where finite-difference approximations to the advection–condensation problem were studied. One-dimensional tests showed that advection of a cloud across the grid results in two numerical artifacts: (i) evaporation of cloud water near the cloud edge, resulting in a distinct temperature undershoots just outside the cloud, and (ii) oscillations in the temperature and moisture variables inside the cloud, near the cloud boundary. The former artifact comes from the advection of cloud water into an undersaturated grid box and its subsequent evaporation. The latter is a consequence of the coupling between temperature and moisture variables, where standard monotonicity constraints considered separately for the temperature and water variables are insufficient to guarantee monotonicity inside the cloud. Grabowski and Smolarkiewicz developed monotonicity constraints for the coupled bulk system and showed that such an approach is relatively straightfor-

* The National Center for Atmospheric Research is sponsored by the National Science Foundation.

Corresponding author address: Wojciech W. Grabowski, NCAR/MMM, P.O. Box 3000, Boulder, CO 80307-3000.
E-mail: grabow@ncar.ucar.edu

ward when applied with the invariant variables (e.g., the total water and liquid water potential temperature).

Accurate prediction of the supersaturation field is the key element of any bin microphysics model. In their simulations of stratocumulus cloud layers, Kogan et al. (1995) observed increased values of the supersaturation near the top of simulated clouds, but they argued that the values were consistent with gravity wave activity combined with radiative cooling near the top. In contrast, Stevens et al. (1996) argued that the two numerical artifacts (i.e., evaporation near cloud edge and overshoots of supersaturation just inside the cloud) were due to spurious processes resulting from application of grid-averaged fields to calculate passage of a cloud front through the grid box. Their key argument (see their Fig. 2) is that advection of a cloud front into a subsaturated grid box (either horizontal or vertical) results first in the evaporation of cloud water to bring the air to saturation and is followed by the nucleation of fresh cloud droplets once the grid box returns to saturation. Stevens et al. (1996) illustrated their argument applying a simple model with an *analytic* representation of advection of thermodynamic variables across a single grid box and showed that the number of nucleated droplets in the second step is determined by the rate of cloud front advection across the grid box (i.e., the local Courant number), and can differ by a factor of 2 from the concentration deeper in the cloud (the latter resulting from the cloud-base nucleation). In general, the Stevens et al. (1996) results suggest a rather pessimistic outlook for high-resolution (large-eddy-simulation type) bin-microphysics modeling of cloud processes and seem to imply that one needs to either explicitly consider subgrid-scale cloud fraction or track the position of cloud interface within the grid box [see Margolin et al. (1997) for the application of the latter approach]. In both cases, processes on cloudy and cloud-free fractions of the grid box need to be considered separately.

The purpose of this paper is to show that the situation is not as hopeless as Stevens et al. (1996) suggest. Our focus is on the spurious cloud-edge supersaturation inside the cloud for two reasons. First, we consider the cloud-edge evaporation as an inherent problem of finite-difference schemes, where numerical diffusion of the advection algorithm is ultimately responsible for the evaporation of cloud water near the cloud edge.¹

¹ A simple approach to cope with this problem is to apply a cloud mask function, whose advection allows recognizing partially cloudy grid boxes where evaporation of cloud water can be disabled. Moreover, when subgrid-scale turbulent diffusion is included in the model physics, evaporation of cloud water near the cloud interface is anticipated (see discussion in Grabowski 2007).

Second, in the context of the bin microphysics, spurious supersaturation near cloud edge can result in additional nucleation of cloud droplets and affect predictions of key cloud properties (such as the effective radius of optical depth), as illustrated in Stevens et al. (1996). The key idea advocated in this paper follows Grabowski (1989): we assume that the supersaturation field is of primary importance and its physically consistent values predicted by the supersaturation equation are to be used as the basis for the adjustment of temperature and humidity fields near the cloud edge.

The next section presents the design of the new approach. The following section discusses 1D tests, similar to those of Grabowski and Smolarkiewicz (1990), applying the two-moment warm-rain microphysics scheme that includes prediction of in-cloud supersaturation (Morrison and Grabowski 2007, 2008). These tests illustrate consistency of the new approach in terms of cloud microphysical properties. The concluding discussion, including addressing application of the new approach to bin microphysics models, is presented in section 4.

2. Description of the approach

Following Grabowski (1989), the main assumption is that it is not the grid-mean supersaturation per se that results in the problem of spurious cloud-edge supersaturation, but rather using the supersaturation derived from grid-mean fields of the temperature T and the water vapor mixing ratio q_v . In a nutshell, we mitigate the problem by adjusting the grid mean T and q_v to the predicted supersaturation, rather than the other way around as in traditional approaches (i.e., when the grid-mean supersaturation is derived from T and q_v). This is in the spirit of Grabowski (1989), with the critical difference that the total water substance is conserved. In this section, we illustrate the approach using a two-moment bulk microphysics approach. As in Morrison and Grabowski (2007, 2008), we consider the coupled system of temperature and moisture equations in the form

$$\frac{d\theta}{dt} = F_\theta, \quad \frac{dq_v}{dt} = F_v, \quad \frac{dq_c}{dt} = F_{qc}, \quad \text{and} \quad \frac{dN_c}{dt} = F_{nc}, \quad (1a), (1b), (1c), (1d)$$

where θ is the potential temperature, q_v is the water vapor mixing ratio, and q_c and N_c are the cloud water mixing ratio and cloud droplet concentration (per unit mass of dry air, i.e., as mixing ratios). The source terms on the right hand side (rhs) may include condensation, radiative cooling, divergence of subgrid-scale fluxes,

etc. Herein, we focus on the advection-condensation problem, and the sources are given by

$$F_{\theta} = \frac{L}{\Pi c_p} C, \quad F_v = -C, \quad F_{q_c} = C, \quad \text{and} \quad F_{n_c} = N, \quad (2)$$

where C is the condensation rate, N is the nucleation rate of cloud droplets (or deactivation rate in case of droplet evaporation), $\Pi = (p/p_0)^{R/c_p}$ is the Exner function (p is the ambient pressure profile, and $p_0 = 1000$ hPa), and L and c_p are the latent heat of condensation and the specific heat at constant pressure. Note that, for simplicity, system (1) is written in the advective form, but the extension to the conservation (flux) form follows from the anelastic continuity equation, where $d\psi/dt \equiv \partial\psi/\partial t + \mathbf{u} \cdot \nabla\psi$ in (1) needs to be replaced by $\partial\psi/\partial t + 1/\rho \nabla(\rho\mathbf{u}\psi)$ (ρ is the air density in the anelastic system and \mathbf{u} is the air velocity). The nucleation rate describes the increase of the number of activated droplets with the increase of the ambient supersaturation; it follows Morrison and Grabowski (2007) and will not be discussed here. The polluted aerosol characteristics from Morrison and Grabowski (2007) are used in tests discussed in the next section (the results for the pristine aerosol are qualitatively similar). For the evaporation, the concentration of droplets does not change unless a complete evaporation of cloud water takes place. It follows that the local source–sink term of droplet concentration, F_{n_c} , is zero except for activation of new cloud droplets and complete evaporation of cloud water. The condensation rate C is given by

$$C = \frac{\delta}{\tau \Gamma(p, T)}, \quad (3)$$

where $\delta \equiv q_v - q_s(p, T)$ is the absolute supersaturation [$q_s(p, T)$ is the water vapor mixing ratio at saturation], $\Gamma(p, T) = 1 + (L/c_p) [dq_s(p, T)/dT]$ is the psychrometric correction, and $\tau = (4\pi D_v N_c \bar{r}_c)^{-1}$ is the relaxation time scale of cloud droplets (\bar{r}_c is the mean radius of cloud droplets, and D_v is the vapor diffusivity in the air).

In the traditional way of solving system (1)–(3), supersaturation is diagnosed from the temperature and water vapor after these fields are updated with advective tendencies together with all forces on the right-hand side of (1a) and (1b) (e.g., Hall 1980; Grabowski 1989). We argue that this is precisely what leads to the problem of spurious cloud-edge supersaturation. Clark (1973) noted that inconsistencies might arise between the supersaturation field updated with advective tendencies of supersaturation combined with physical forces, and the supersaturation diagnosed from temperature and water vapor fields in the traditional ap-

proach. However, as shown in the next section, addressing this inconsistency by adjusting the temperature and water vapor fields to the predicted supersaturation is necessary but not sufficient to remove the spurious cloud-edge supersaturation; advection of the supersaturation with a monotonic scheme is also required. We propose to use the solution of the supersaturation equation (calculated with a monotonic advection scheme) to adjust solutions of the temperature and water vapor equations. The following discussion explains this approach in more detail.

Equations (1a), (1b), and (3), together with the hydrostatic balance $dp/dz = -\rho g$, lead to the following evolution equation for the absolute supersaturation:

$$\frac{d\delta}{dt} = wg \left(\rho \frac{\partial q_s}{\partial p} + \frac{1}{c_p} \frac{\partial q_s}{\partial T} \right) - \frac{\delta}{\tau}. \quad (4)$$

A general form of (4), including other forces for the temperature and moisture, is presented in Morrison and Grabowski [2008; Eq. (A8) therein]. The first term on rhs represents forcing due to the vertical velocity (all other explicit forces in the temperature and moisture equations are set to zero here), whereas the last term represents the tendency due to condensational growth of cloud droplets. The solution of (4) represents a physically consistent prediction of the supersaturation. In contrast, diagnosing supersaturation from solutions of (1a) and (1b) introduces errors and the solutions of the temperature and moisture equations need to be adjusted to produce a supersaturation that matches the solution of (4). It follows that the modified scheme first solves (1) and subsequently adjusts the solutions to match the updated supersaturation given by solution of (4). The adjustment can be schematically written as

$$q_v = q_v^* - \epsilon, \quad q_c = q_c^* + \epsilon, \quad \text{and} \quad \theta = \theta^* + \frac{L}{\Pi c_p} \epsilon, \quad (5)$$

where variables with and without the asterisk represent solutions of (1a)–(1c) and the adjusted solutions, respectively; and ϵ is the mixing ratio of cloud water that has to condense (if $\epsilon > 0$) or evaporate (if $\epsilon < 0$) to make temperature and moisture fields matching the predicted supersaturation. The latter is obtained by solving the following (nonlinear) equation:

$$\delta^* = q_v^* - \epsilon - q_s \left(p, T^* + \frac{L}{c_p} \epsilon \right), \quad (6a)$$

where δ^* is the absolute supersaturation updated using (4). In subsaturated conditions, the adjustment is limited so that $\epsilon \leq 0$, to prevent spurious generation

of cloud water outside of the cloud. Moreover, ϵ derived from (6a) has to be limited by the available cloud water q_c^* :

$$\epsilon = \max(-q_c^*, \epsilon). \quad (6b)$$

Since values of ϵ required for the adjustment (5) are typically small, it is sufficient to use the linearized version of (6a). In such a case ϵ can be derived analytically as

$$\epsilon = \frac{q_v^* - q_s(p, T^*) - \delta^*}{\Gamma(p, T^*)}. \quad (7)$$

Tests discussed in the next section illustrate that using (7) is sufficient.

In summary, in the modified approach, the supersaturation equation is solved in addition to the temperature and moisture equations, and its solution is used to adjust the solutions for temperature and moisture according to (5) and (7).

3. Computational examples

Developments discussed in the previous section are illustrated using an idealized one-dimensional problem, similar to Grabowski and Smolarkiewicz (1990). We apply a nonoscillatory forward-in-time (NFT) approach based on the one-dimensional version of finite-volume-wise transport scheme MPDATA (Smolarkiewicz 1984; Smolarkiewicz and Clark 1986; Smolarkiewicz and Grabowski 1990; see Smolarkiewicz and Margolin 1998 for a review). In the following discussion, we use the semi-Lagrangian form of equations for the illustration of numerical details, thereby simplifying the notation. The system (1) and Eq. (4) are examples of a general equation,

$$\frac{d\psi}{dt} = F. \quad (8)$$

If (8) is to be solved using uncentered-in-time integration scheme, then the solution (at every model grid point) can be written as

$$\psi^{n+1} = (\psi^n + \Delta t F^n)|_0, \quad (9)$$

where superscripts n and $n + 1$ represent time levels, the symbol $|_0$ is shorthand for mapping the field value to the departure point of the flow trajectory arriving at (x_i, t^{n+1}) grid point. Because there is no ambiguity, the grid location index has been dropped on both sides of (9). Once ψ^{n+1} is derived using (9), the force at $n + 1$ time level F^{n+1} can be derived and applied in (9) during the next time step. When the adjustment discussed in the previous section is used, (9) is applied to system (1)

and (4) to obtain provisional variables ψ^* (i.e., θ^* , q_v^* , q_c^* , and δ^*). These are subsequently adjusted using (5) and (7), before F^{n+1} are calculated.

The uncentered-in-time scheme detailed above is used in the examples discussed below. It is straightforward to extend the above scheme to the centered-in-time scheme, where (9) is replaced by

$$\psi^{n+1} = \left(\psi^n + \frac{1}{2} \Delta t F^n \right) \Big|_0 + \frac{1}{2} \Delta t F^{n+1}. \quad (10)$$

One approach is to apply the predictor-corrector technique, where the uncentered-in-time scheme (9) is first used to obtain forces F at $n + 1$ time level, and these are subsequently used in the centered-in-time scheme (10). In such a case, the adjustment (5) and (7) needs to be applied twice: the first time in the predictor step, and the second time to adjust the centered-in-time solutions.

To illustrate the theoretical considerations, we present solutions to idealized one-dimensional advection-condensation problems, similar to the one considered in Grabowski and Smolarkiewicz (1990). A square wave perturbation of the temperature and water vapor is advected either vertically or horizontally with a constant velocity in the environment characterized by the uniform profile of the temperature (lapse rate of -6 K km^{-1}) and constant relative humidity of 50%. The extent of the integration domain is 600 m, and an initial perturbation (100-m extent) is placed near the bottom of the domain. The initial potential temperature perturbation is 1 K. For the vertical advection, the initial moisture perturbation is such that the relative humidity is 99.8%. It follows that cloud droplets are first nucleated (maximum relative supersaturation is expected to be around 0.2%, resulting in nucleation of about 550 mg^{-1} of cloud droplets²) and they subsequently grow during the ascent. For the horizontal advection, the initial moisture perturbation includes 1 g kg^{-1} of cloud water and the relative humidity is 100.15% (i.e., the relative supersaturation is below the maximum value in the vertical test). Initial droplet concentration is set to that nucleated in the vertical test (550 mg^{-1}). For the horizontal advection, the initial supersaturation inside a cloud is supposed to diminish due to the growth of cloud droplets. The pressure is 800 hPa for the horizontal advection test, and $p(z = 0) = 800 \text{ hPa}$ in the vertical advection test. The spatial resolution is 2 m and the velocity (either vertical or horizontal) is 1 m s^{-1} . The

² It is convenient to express droplet concentration in units of mg^{-1} , that is, 10^{-6} kg^{-1} , because this value approximately corresponds to the volume concentration expressed in cm^{-3} .

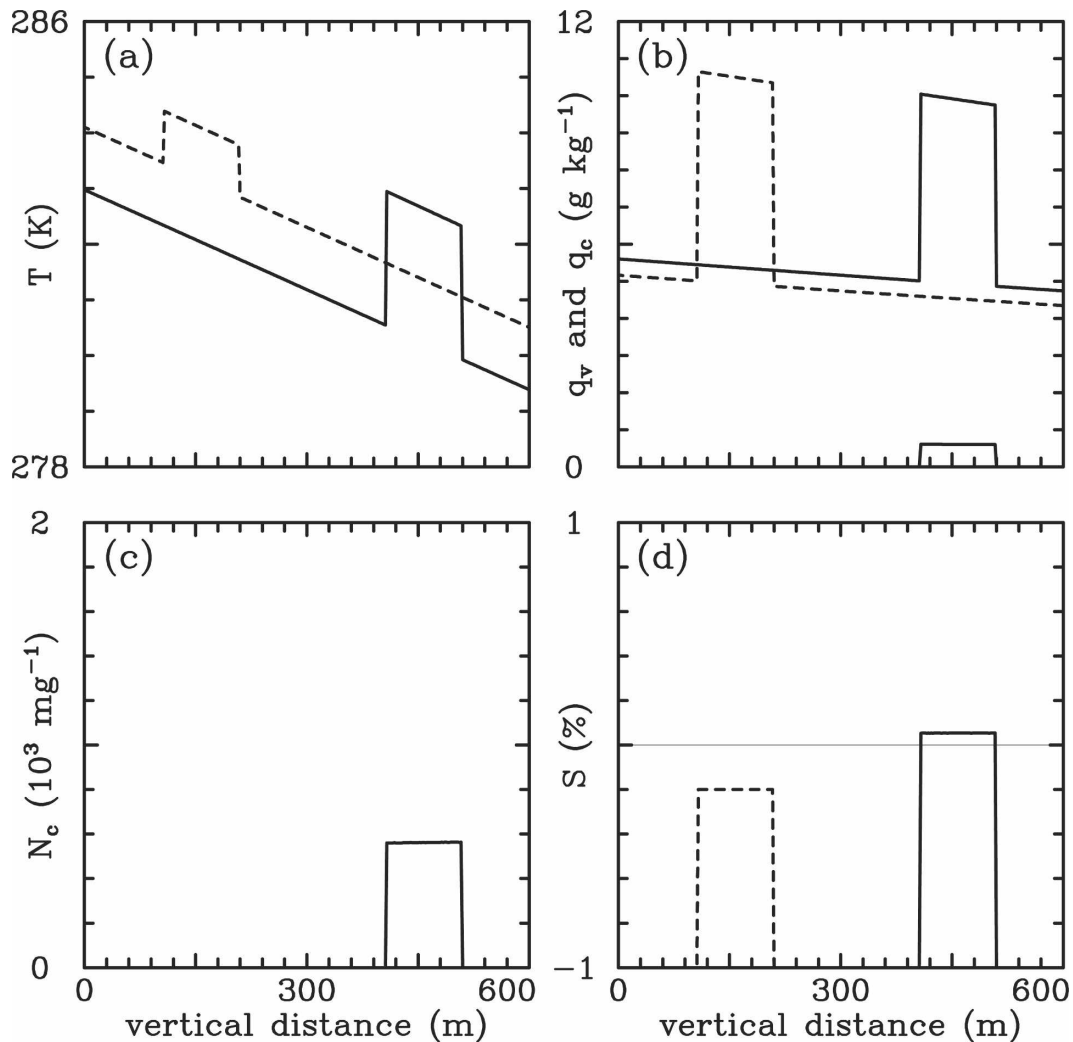


FIG. 1. Quasi-analytic solution to the vertical advection-condensation problem. Profiles of the (a) temperature, (b) water vapor and cloud water mixing ratios, and (c) concentration of cloud droplets and relative supersaturation $S = \delta/q_s$ at $t = 0$ (dashed line) and $t = 300$ s (solid line).

results are presented after 300 s, which is equivalent to 300 m in the displacement of the initial perturbation.

Figure 1 illustrates the solution to the vertical advection-condensation test obtained using the 2-s time step that results in the exact advection of the initial perturbation (i.e., the Courant number of 1). Since the nucleation of cloud droplets and their condensational growth is calculated numerically as in other tests, we refer to this solution as quasi-analytic. The test shows vertical advection of the initially subsaturated square-wave perturbation, nucleation of cloud droplets, and their subsequent growth. As expected, condensation increases the initial temperature perturbation and slightly reduces the water vapor mixing ratio within the perturbation. The final relative supersaturation within the perturbation is around 0.05%.

Figure 2 shows corresponding solution obtained using a traditional approach to solving system (1) (i.e., when the supersaturation is diagnosed using predicted temperature and moisture) applying a time step of 0.2 s and the monotone advection scheme. For several reasons, we purposely select a relatively short time step (Courant number of 0.1) for all subsequent tests. First, cloud edges are likely to be advected at relatively low Courant numbers because their velocities are typically significantly smaller than the maximum velocity within a simulated cloud, the latter dictating the time step applied in the simulation. Second, MPDATA becomes less accurate at low Courant numbers, and the results shown here improve when a larger time step is used. Finally, the uncentered-in-time approach used in a particular implementation applied herein is best suited for

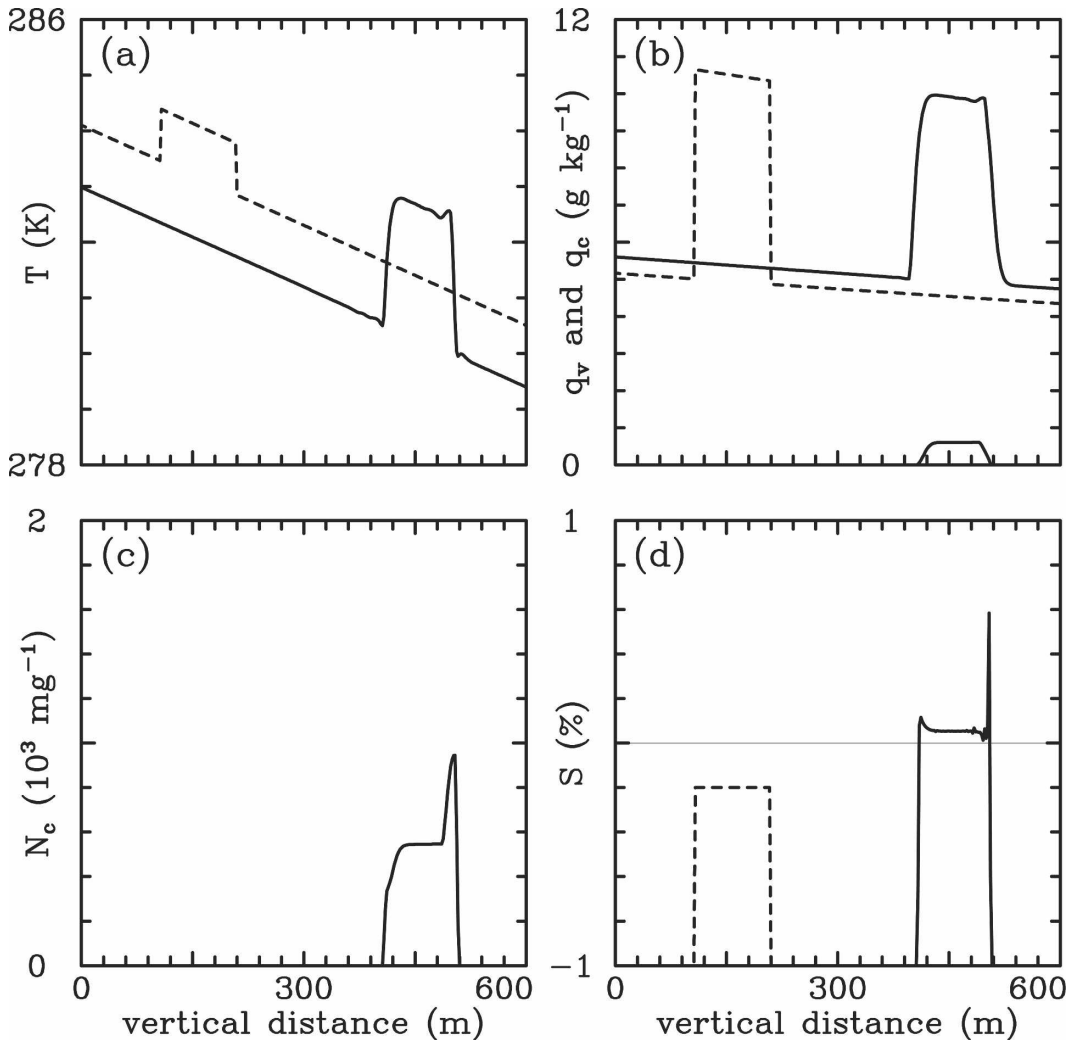


FIG. 2. As in Fig. 1, but for the solution with $\Delta t = 0.2$ s (Courant number of 0.1) applying the traditional approach. Advection scheme applies the monotone option.

short time steps. The bulk properties of the solution (the temperature, water vapor, and cloud water mixing ratios) are consistent with the quasi-analytic solution. However, the supersaturation field shows a significant overshoot at the leading edge, which results in additional nucleation of cloud droplets. This is precisely the problem reported in Grabowski (1989) and further explored in Stevens et al. (1996).

Results with additional adjustment of temperature and moisture fields to match the solution of the supersaturation equation are shown in Fig. 3. Clearly, the leading-edge supersaturation shows only minimal overshoot (comparable to that at the trailing edge) and the droplet concentration agrees with the quasi-analytic solution. Apparently, the small overshoots near cloud edges do not lead to additional nucleation. The presence of these overshoots is related to the spatial vari-

ability of the phase relaxation time scale τ (due to numerical diffusion), which changes from a finite value inside the cloud to infinity in cloud-free air. This is supported by tests with $\tau = \text{const}$ in which these overshoots are absent (not shown).

It is important to note that the adjustment illustrated in Fig. 3 has a negative impact on the buoyancy field near the interface: the temperature and water vapor fields in Figs. 3a and 3b show stronger oscillations near the interface than in corresponding panels of Fig. 2. In the quasi-analytic solution (Fig. 1), the buoyancy perturbation associated with the temperature and moisture perturbations between approximately 400 and 500 m at $t = 300$ s corresponds to the density temperature perturbation of about 2.2 K. The overshoots at the leading edge of the perturbation in the traditional approach (Fig. 2) correspond to the density temperature of about

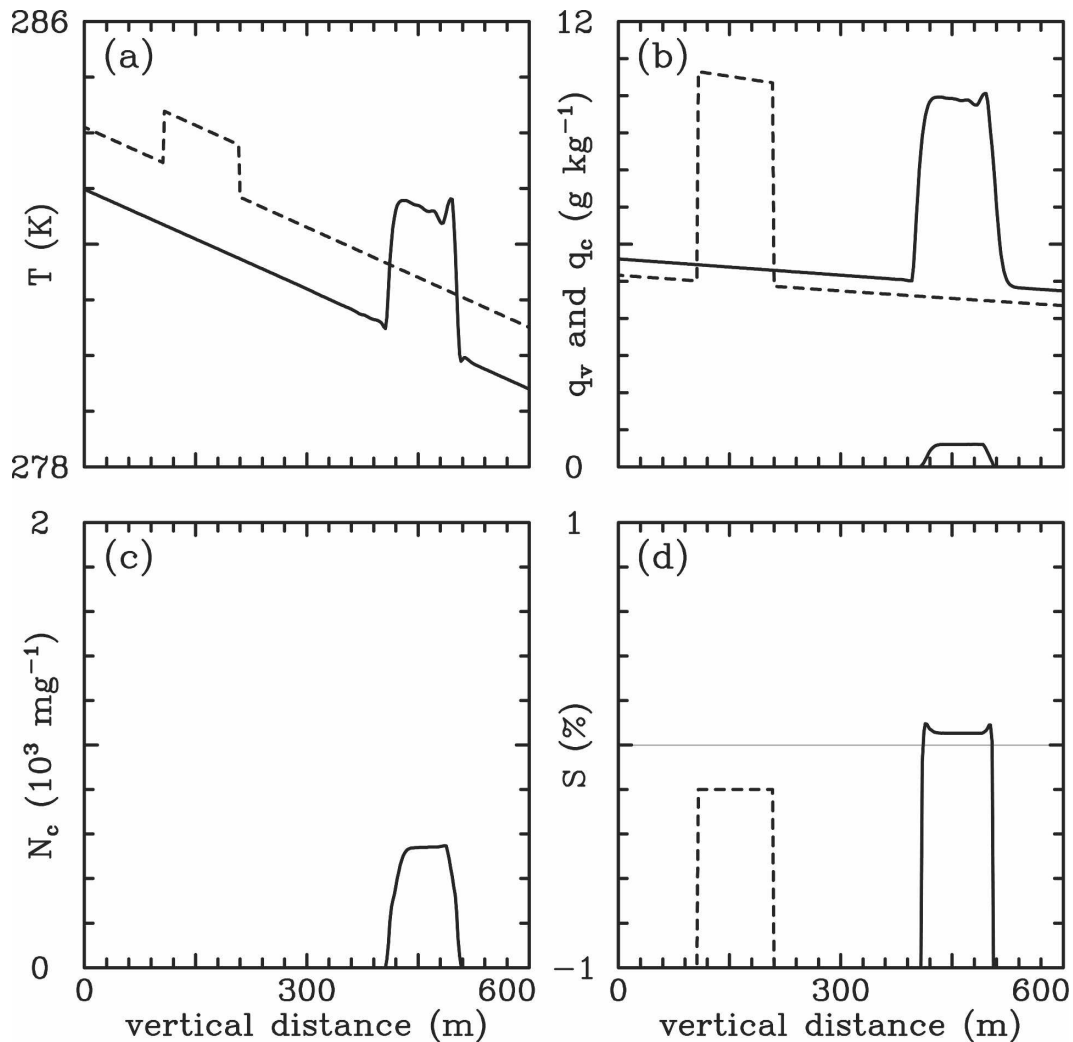


FIG. 3. As in Fig. 2, but with the approach advocated in this paper.

2.4 K, that is, about 10% overshoot. When the approach advocated in this paper is used (Fig. 3), the maximum buoyancy corresponds to the density temperature of about 2.7 K, that is, about 20% overshoot. Arguably, presence of these overshoots can have a negative impact on simulations using a dynamic model, and the adjustment advocated here might strengthen such an impact. However, the presence of the parameterized mixing due to subgrid-scale turbulence will tend to weaken these overshoots. In fact, no adverse effects were observed in the rising thermal simulations reported in Morrison and Grabowski (2008) when the approach proposed here was applied.

It needs to be stressed that both the monotonicity of the advection scheme and the adjustment advocated here need to be utilized to avoid microphysical artifacts. This is illustrated in Fig. 4, which shows results

obtained when neither the monotonicity nor the adjustment are enforced. The deterioration of the numerical solution is obvious: strong oscillations inside the perturbation result in the buoyancy oscillations with the maximum density temperature of 3.3 K, that is, approximately 50% overshoot compared to the quasi-analytic solution. When the adjustment is combined with the nonmonotone scheme (not shown), the solution improves to some extent compared to the one in Fig. 4, but significant oscillations remain in all fields.

Results of the horizontal advection tests are shown in Figs. 5 and 6. The quasi-analytic solution for this case (not shown) represents exact advection of the initial perturbation, with initial supersaturation perturbation quickly approaching zero and a corresponding small increase of the temperature and cloud water, and decrease of the water vapor. In the horizontal advection

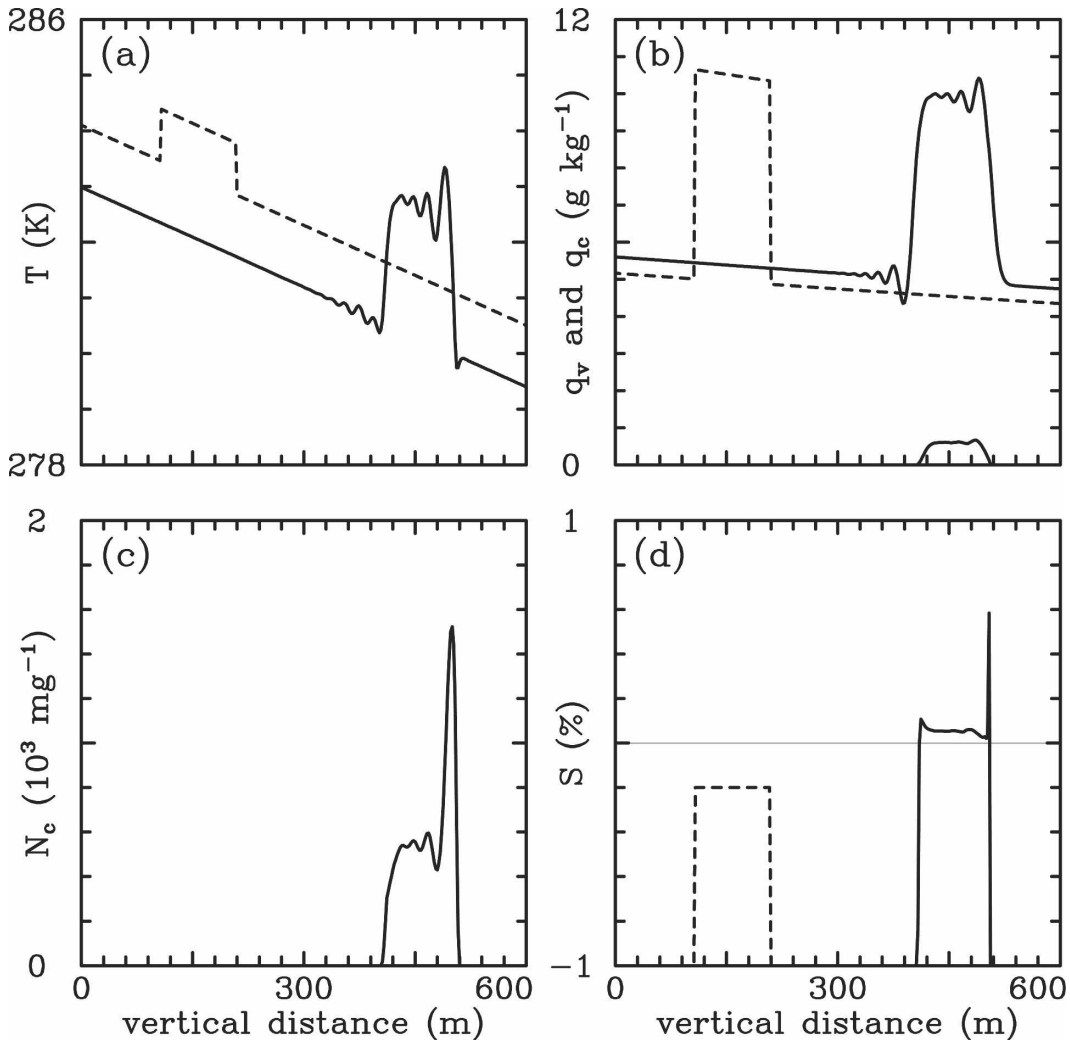


FIG. 4. As in Fig. 2, but without the monotone option of the advection scheme.

test, the temperature and water mixing ratios (Figs. 5a,b and 6a,b) remain monotone inside the cloud because the monotone advection scheme is used and the forcing term in the supersaturation equation vanishes as $w \equiv 0$. Moreover, the temperature undershoots outside the cloud, resulting from evaporation of cloud water, are significantly stronger than in the vertical test. Figure 5 shows results when the traditional approach is used, that is, when the supersaturation is diagnosed using predicted temperature and moisture. In this case, the leading-edge overshoot of the supersaturation results in the additional nucleation of cloud droplets, similarly to the vertical tests, and in agreement with the discussion in Stevens et al. (1996). Applying the adjustment (Fig. 6) removes this overshoot and results in smooth fields of the temperature, moisture, droplet concentration, and supersaturation inside the cloud.

4. Discussion and conclusions

This paper presents a simple approach to mitigate the spurious cloud-edge supersaturation in cloud models. The main point, following Grabowski (1989), is that the supersaturation diagnosed from solutions of the temperature and water vapor equations is *not monotone* inside the cloud even if a monotone advection scheme is used for solutions of the temperature and moisture equations. This is because of the nonlinear coupling between the temperature and moisture. The approach advocated in this paper is to solve independently the equation governing the evolution of the supersaturation, and adjust temperature and moisture solutions in such a way that they provide supersaturation consistent with the one obtained from the supersaturation equation. Computational examples illustrate that the pro-

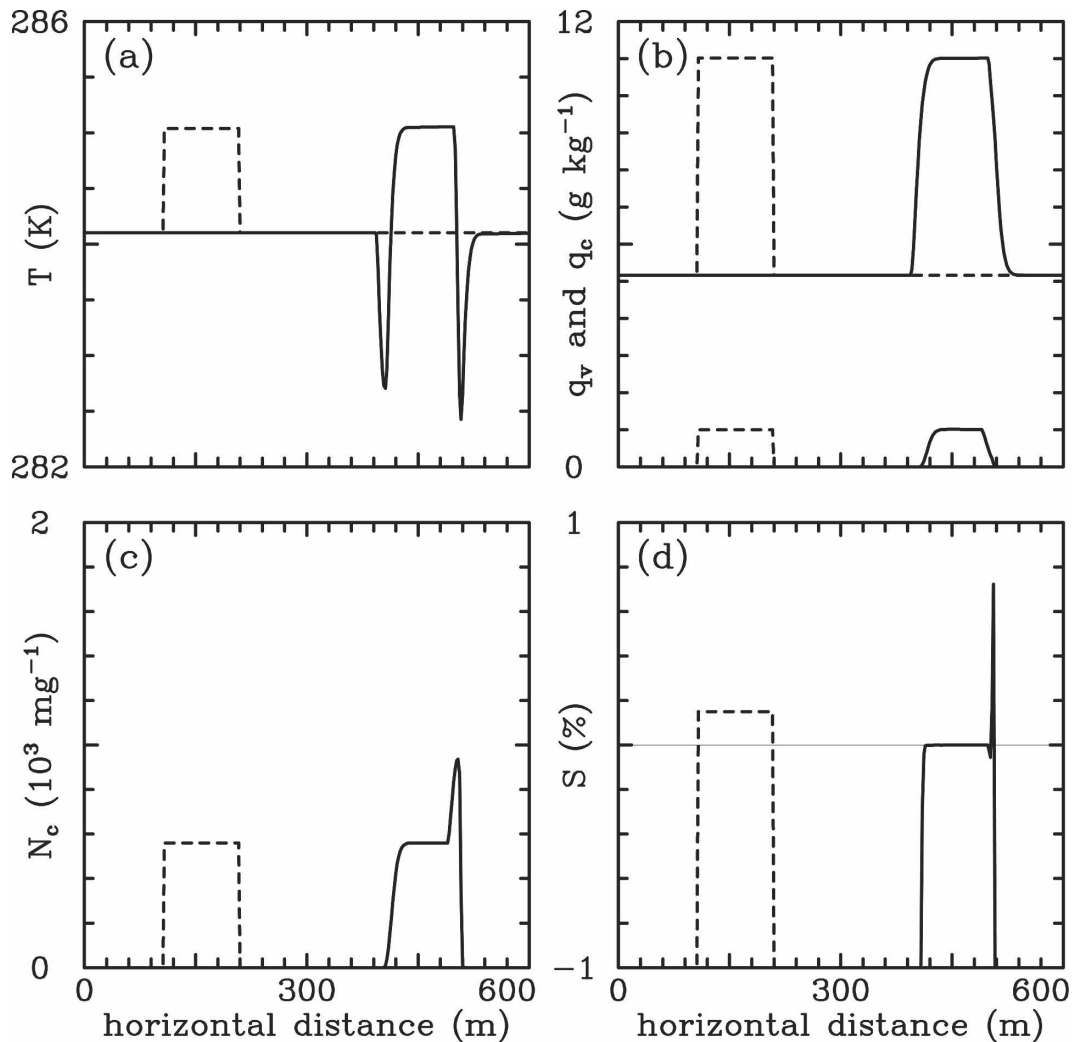


FIG. 5. As in previous figures, but for the solution to the horizontal advection–condensation problem with $\Delta t = 0.2$ s (Courant number of 0.1) and applying the traditional approach. Advection scheme applies the monotone option.

posed approach results in consistent fields of both macroscopic (temperature and mixing ratios) and microscopic variables (concentration of cloud droplets and supersaturation). This is in contrast to a rather pessimistic argument put forward by Stevens et al. (1996). The key point is that the monotone advection scheme and the adjustment proposed here are both required to obtain an improved supersaturation field and mitigate spurious droplet nucleation. However, the adjustment does worsen the temperature and moisture fields near the interface, and hence it has a negative impact on the buoyancy field. Because the region of the cloud edge is typically where the subgrid-scale turbulent diffusion is active, this aspect is arguably not as critical as having the physically consistent supersaturation field (see ris-

ing thermal simulations in Morrison and Grabowski 2008).

Models predicting supersaturation typically apply bin microphysics, where a few tens of size bins are used to describe the shape of the cloud droplet spectrum. It follows that the main problem for such models is how to distribute the adjustment amount ϵ into the model bins. In general,

$$\epsilon = \sum_{i=1}^N \epsilon_i, \quad (11)$$

where ϵ_i is the adjustment for bin i , and N is the total number of bins. Because the condensation rate is inversely proportional to the relaxation time scale τ [see

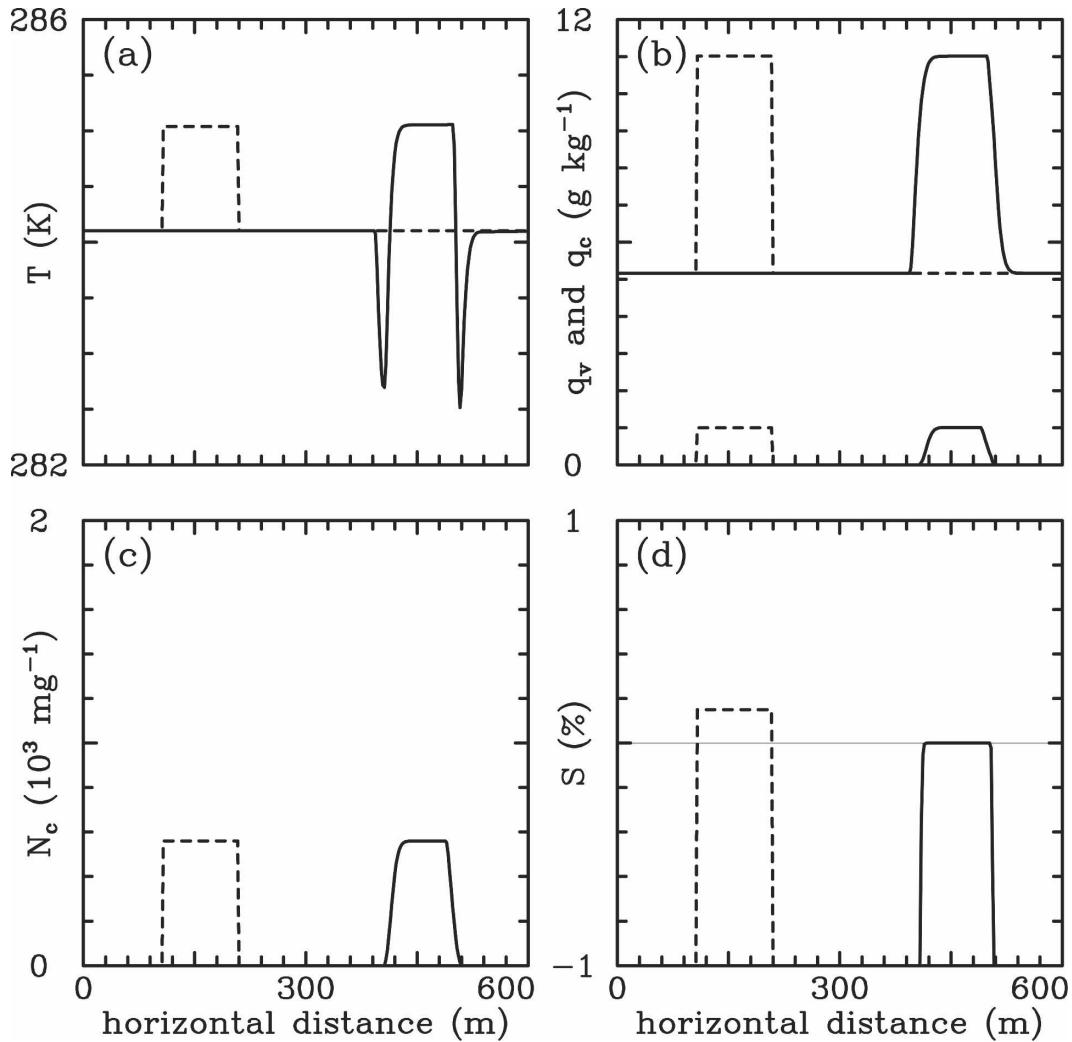


FIG. 6. As in Fig. 5, but with the approach advocated in this paper.

(3)], the adjustment for bin i should be inversely proportional to the relaxation time scale τ_i characterizing droplets in this bin. It follows that

$$\epsilon_i = \frac{\epsilon}{\beta\tau_i}, \quad \text{where} \quad \beta = \sum_{k=1}^N \frac{1}{\tau_k}. \quad (12)$$

However, (12) does not allow a straightforward prediction of the change of the spectral density function that is typically used in bin models (e.g., Kogan et al. 1995 and references therein; Morrison and Grabowski 2007). To address this issue, one can use a “dummy” value of supersaturation, $\delta' = \tau\Gamma\epsilon$ [cf. (3)], applied to the spectral density function to calculate its change during the adjustment (i.e., treating the adjustment as a condensation/evaporation process). The resulting change in the spectral density function produces a change in the

bulk cloud water (i.e., integrated over the size spectrum) equal to ϵ , as required by (5) and (7).

Finally, the same approach should be applied in models that include ice processes. Physically consistent prediction of the supersaturation field in such models may be especially important given the complexity associated with mixed-phase conditions. However, additional considerations must be taken into account in order to partition the total adjustment ϵ between liquid and ice. This aspect is left for future research.

Acknowledgments. This work was supported by the NOAA Grant NA05OAR4310107 and by the NSF Science and Technology Center for Multi-Scale Modeling of Atmospheric Processes (CMMAP), managed by Colorado State University under Cooperative Agreement ATM-0425247.

REFERENCES

- Clark, T. L., 1973: Numerical modeling of the dynamics and microphysics of warm cumulus convection. *J. Atmos. Sci.*, **30**, 857–878.
- Grabowski, W. W., 1989: Numerical experiments on the dynamics of the cloud-environment interface: Small cumulus in a shear-free environment. *J. Atmos. Sci.*, **46**, 3513–3541.
- , 2007: Representation of turbulent mixing and buoyancy reversal in bulk cloud models. *J. Atmos. Sci.*, **64**, 3666–3680.
- , and P. K. Smolarkiewicz, 1990: Monotone finite difference approximations to the advection-condensation problem. *Mon. Wea. Rev.*, **118**, 2082–2097.
- Hall, W. D., 1980: A detailed microphysical model within a two-dimensional framework: Model description and preliminary results. *J. Atmos. Sci.*, **37**, 2486–2507.
- Klaassen, G. P., and T. L. Clark, 1985: Dynamics of the cloud-environment interface and entrainment in small cumuli: Two-dimensional simulations in the absence of ambient shear. *J. Atmos. Sci.*, **42**, 2621–2642.
- Kogan, Y. L., M. P. Khairoutdinov, D. K. Lilly, Z. N. Kogan, and Q. Liu, 1995: Modeling of stratocumulus cloud layers in a large eddy simulation model with explicit microphysics. *J. Atmos. Sci.*, **52**, 2923–2940.
- Margolin, L., J. M. Reisner, and P. K. Smolarkiewicz, 1997: Application of the volume-of-fluid method to the advection-condensation problem. *Mon. Wea. Rev.*, **125**, 2265–2273.
- Morrison, H., and W. W. Grabowski, 2007: Comparison of bulk and bin warm-rain microphysics models using a kinematic framework. *J. Atmos. Sci.*, **64**, 2839–2861.
- , and —, 2008: Modeling supersaturation and subgrid-scale mixing in a large-eddy model with two-moment bulk warm microphysics. *J. Atmos. Sci.*, **65**, 792–812.
- Smolarkiewicz, P. K., 1984: A fully multidimensional positive definite advection transport algorithm with small implicit diffusion. *J. Comput. Phys.*, **54**, 325–362.
- , and T. L. Clark, 1986: The multidimensional positive definite advection transport algorithm: Further development and applications. *J. Comput. Phys.*, **67**, 396–438.
- , and W. W. Grabowski, 1990: The multidimensional positive definite advection transport algorithm: Nonoscillatory option. *J. Comput. Phys.*, **86**, 355–375.
- , and L. G. Margolin, 1998: MPDATA: A finite-difference solver for geophysical flows. *J. Comput. Phys.*, **140**, 459–480.
- Stevens, B., R. L. Walko, and W. R. Cotton, 1996: The spurious production of cloud-edge supersaturation by Eulerian models. *Mon. Wea. Rev.*, **124**, 1034–1041.